

Neutron irradiation effects in chemical-vapor-deposited diamond

A. E. Karkin,^{1,*} V. I. Voronin,¹ I. F. Berger,² V. A. Kazantsev,¹ Yu. S. Ponosov,¹ V. G. Ralchenko,³ V. I. Konov,³ and B. N. Goshchitskii¹¹*Institute of Metal Physics UB RAS, S. Kovalevskoi Strasse 18, Ekaterinburg 620219, Russia*²*Institute of Solid State Chemistry UB RAS, Pervomaiskaya Strasse 91, Ekaterinburg 620219, Russia*³*A.M. Prokhorov General Physics Institute RAS, Vavilov Strasse 38, Moscow 119991, Russia*

(Received 15 April 2008; published 30 July 2008)

The structural disorder, heat capacity, resistivity, Hall effect, and magnetic susceptibility of polycrystalline chemical-vapor-deposited diamond irradiated with fast neutrons at temperature of (325 ± 10) K at high fluences $\Phi = (1-5) \times 10^{20} \text{ cm}^{-2}$ were investigated. Despite a significant increase in unit-cell volume ($\sim 4.5\%$), the crystalline structure remains stable in this fluence range. The irradiation results in a paramagnetic contribution to magnetic susceptibility and to a strong (by 4 orders of magnitude) increase in heat capacity at low temperatures ($T < 20$ K) due to electron contribution with a T dependence characteristic of multilevel electron systems (the Schottky anomaly).

DOI: 10.1103/PhysRevB.78.033204

PACS number(s): 61.82.Fk, 65.40.Ba, 72.20.My, 75.20.Ck

Disordering induced by irradiation with fast neutrons and other high-energy particles is used not only for deep modification of physical properties of material via significant nano-scale restructuring but also as a method of initial (ordered)-state investigation.¹ Different forms of carbon, such as graphite, diamond, nanotubes, fullerenes, and graphene, feature a number of unique properties promising for advanced applications. Carbon, with its great variety of structures and bonding type, including sp^1 , sp^2 , and sp^3 bonding, is especially interesting for study of different radiation-induced structure transformations,² the graphite-to-diamond transition³ being a good example.

Diamond, in particular, presents a promising wide energy-gap material for electronic devices,^{4,5} due to its extraordinary properties (record high thermal conductivity, radiation hardness, and high charge-carrier mobility) and superconductivity recently discovered in boron-doped samples.^{6,7} Earlier studies of the effect of radiation disordering on the physical properties of diamond may be conditionally divided into two groups. The first one includes experiments, mainly optical,⁸ on irradiation with relatively low fluences Φ being carried out for over 50 years and often connected with the study of color change of natural diamonds. The concentration of radiation defects in this case is commensurable with that of natural defects and, in different estimates, does not exceed 0.1%. The second group includes irradiation with relatively high fluences, when a maximum possible concentration of defects (equilibrium at the given irradiation temperature) is realized. These are optical experiments on single-crystal diamonds exposed to ion irradiation with a few MeV energy^{9,10} and investigations on natural diamond powders irradiated with fast neutrons.¹¹⁻¹⁶ The fast neutron irradiation experiments were carried out at elevated (~ 500 °C) (Ref. 11) or uncontrolled¹²⁻¹⁶ sample temperatures, which, in fact, predetermined the observed radiation effects: the transition from diamond to graphite-type structure and accordingly, the very strong decrease (up to 40%) in the sample mass density.

The purpose of the present work was to perform complex characterization (neutron and Raman scattering and evaluation of heat capacity and electrical and magnetic properties) of diamond irradiated with fast neutrons at well-controlled

irradiation temperature $T_{\text{irr}} = (325 \pm 10)$ K, which is below the characteristic temperature (≈ 650 K) for point defect diffusion activation.¹⁰ One of the unexpected results of the investigation is a revelation in irradiated samples of the significant electronic contribution to low-temperature heat capacity.

The samples were unpolished translucent plates of polycrystalline chemical-vapor-deposited (CVD) diamond grown on a Si substrate in a microwave plasma in CH_4/H_2 mixture.¹⁷ The plates were laser cut from a single freestanding diamond wafer to $4.0 \times 2.5 \times 0.45 \text{ mm}^3$ size. The dimensions of crystallites at the growth side were 80–100 μm . The CVD diamond does not contain metallic impurities inherent to synthetic high-pressure high-temperature (HPHT) diamonds. It was found from optical-absorption spectra that the principal impurities in the samples were nitrogen (1.7 ± 0.2 ppm) and hydrogen (80 ± 10 ppm).

Irradiation with fast neutrons (flux of $\sim 10^{14} \text{ cm}^{-2} \text{ s}^{-1}$, energies of over 0.1 MeV) to fluences $\Phi = 1, 2, 3$ and $5 \times 10^{20} \text{ cm}^{-2}$ was carried out in the wet channel of the IVV-2M nuclear reactor at INP. The samples were sealed in thin (50 μm) aluminum foil to minimize their heating during the irradiation. Neutron-diffraction measurements were performed in a horizontal channel of the reactor (1.532 Å wavelength) at room temperature. Other analysis included: (i) magnetic measurements in the Quantum Design superconducting quantum interference device (SQUID) magnetometer in the temperature range $T = (2-200)$ K in magnetic fields up to 5 T; (ii) heat-capacity measurements in the physical properties measurement system (PPMS) unit at $T = (2-300)$ K; (iii) Raman scattering with a Renishaw spectrometer (514 nm excitation wavelength) at room temperature; and (iv) resistivity and Hall-effect measurements by a four-contact method at $T = (260-380)$ K in the field up to 13.6 T.

The neutron-diffraction patterns for as-grown and irradiated at fluence $\Phi = 3 \times 10^{20} \text{ cm}^{-2}$ diamond samples are shown in Fig. 1. The principal effect of the irradiation consists of a considerable increase in lattice parameter (the change in unit-cell volume, $\Delta V/V$) and an increase in Debye-Waller factor B . However, a broadening in the diffraction lines is absent within the experimental accuracy (0.01° at

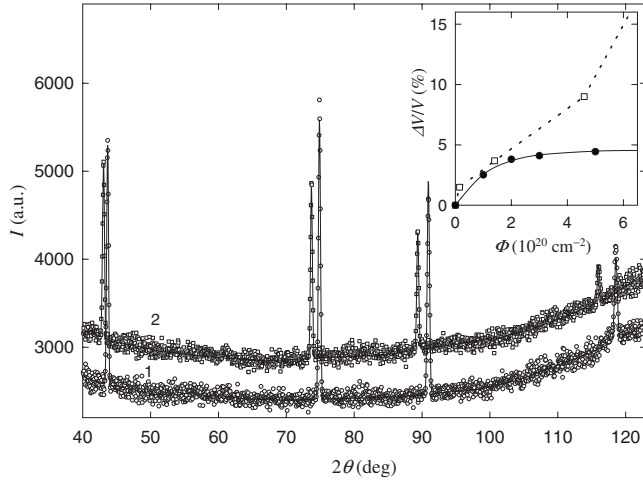


FIG. 1. Neutron-diffraction patterns for as-grown (1) and irradiated to fluence $\Phi=3 \times 10^{20} \text{ cm}^{-2}$ (2) diamond samples. The symbols are experimental data; the solid line is fitting with a FULLPROF program. Inset: unit-cell volume increase, $\Delta V/V$, vs Φ . The full circles are our data, the solid line is fitting with Eq. (1), and the open squares and dashed line are the data from Ref. 14.

angle $2\theta \sim 95^\circ$). Thus, our results differ from those reported in Refs. 12, 13, and 16, where broad halos were observed in the diffraction patterns of irradiated diamonds, which corresponded to formation of nanocrystalline or amorphous material.

The relative increase in unit-cell volume, $\Delta V/V$, as a function of Φ shows a saturation effect at $\Phi \geq 2 \times 10^{20} \text{ cm}^{-2}$ and is described with a simple formula:

$$\Delta V/V = a[1 - \exp(-\Phi/\Phi_0)], \quad (1)$$

where the parameter $a = (4.5 \pm 0.1)\%$ and $\Phi_0 = (1.2 \pm 0.1) \times 10^{20} \text{ cm}^{-2}$. The similar saturation effect is indicative for other properties (magnetization, thermal capacity, and resistivity). The parameter B increases to $(1.8 \pm 0.3) \text{ \AA}^2$ for $\Phi = 5 \times 10^{20} \text{ cm}^{-2}$, which corresponds to the rms value of atomic displacements $(\langle u^2 \rangle)^{1/2} \approx 0.16 \text{ \AA}$, or about 10% of the interatomic distance (1.54 \AA).

While in the initial state diamond is a diamagnetic with $\chi_0 = -(1.15 \pm 0.05) \times 10^{-6}$, a paramagnetic contribution of Curie-Weiss type $\chi = \chi_0 + C/(T+T_0)$ appears after irradiation (Fig. 2), with no measurable dependence of χ on the magnetic field within 1–5 T. The χ_0 value is approximately the same as for the as-grown sample, $\chi_0 = -(1.1 \pm 0.2) \times 10^{-6}$, $T_0 \approx 5 \text{ K}$. The Curie constant $C \approx 0.8 \text{ K}$, which corresponds (for $\frac{1}{2}$ spin) to concentrations of paramagnetic centers $c_{\text{PM}} = 0.8\%$ and 0.7% for samples irradiated to fluences of 2×10^{20} and $5 \times 10^{20} \text{ cm}^{-2}$, respectively.

The paramagnetism, as well as ferromagnetism, was observed earlier in many carbon forms. For example, a ferromagnetic behavior was observed in nanosized diamond particles irradiated with 100 keV ions¹⁸ and in pyrolytic graphite irradiated with 2.25 MeV protons,¹⁹ while paramagnetism has been reported for diamond irradiated with fast neutrons,^{20,21} multiwalled nanotubes irradiated with 2.5-MeV electrons,²² and “carbon foam.”²³

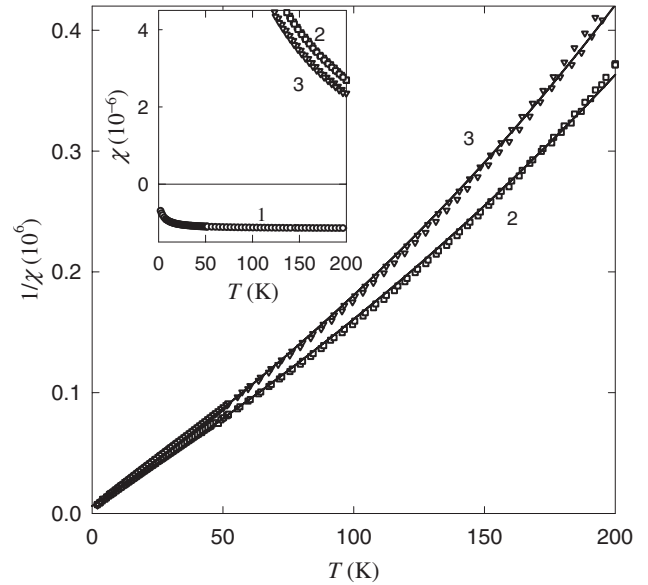


FIG. 2. Temperature dependences of direct (χ , inset) and reciprocal ($1/\chi$) magnetic susceptibility of CVD diamond: as-grown sample (1) and the samples irradiated to fluences $\Phi=2 \times 10^{20}$ (2) and $5 \times 10^{20} \text{ cm}^{-2}$ (3).

Shown in Fig. 3 is heat capacity c_V of the reference sample and the sample irradiated to fluence $\Phi=5 \times 10^{20} \text{ cm}^{-2}$. A considerable (4 orders of magnitude at helium temperature) increase in low-temperature heat capacity in the irradiated sample related, obviously, to the appearance of an electron contribution is worth special notice.

This contribution has the shape of a broad peak which is noticeably broader than the Schottky anomaly corresponding to a simple two-level system. Let us represent the total thermal capacity as phonon and electron contributions:

$$c_V = c_{\text{ph}} + c_{\text{el}}. \quad (2)$$

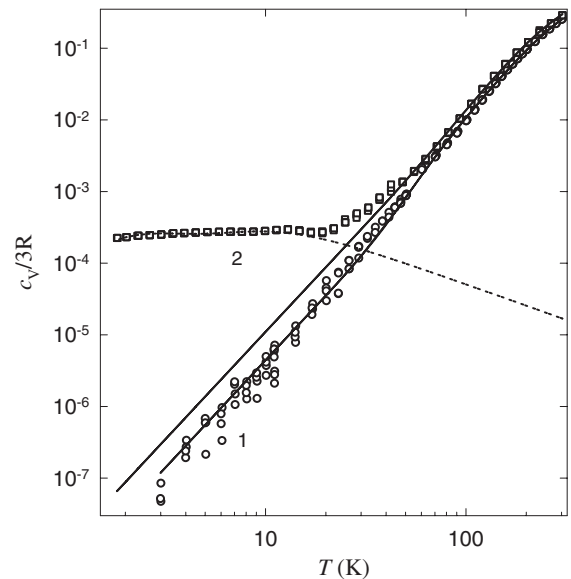


FIG. 3. Temperature dependence of heat capacity $c_V/3R$ for as-grown (1) and irradiated to fluence $\Phi=5 \times 10^{20} \text{ cm}^{-2}$ diamond sample (2). The solid and dashed lines show the phonon and electron contributions, respectively.

For simplicity, we represent the phonon contribution in the form of two Debye steps with frequencies cut off at θ_1 and θ_2 ,

$$c_{\text{ph}}/3R = a_1 D(\theta_1/T) + a_2 D(\theta_2/T), \quad a_1 + a_2 = 1, \quad (3)$$

where $D(x)$ is the Debye function, $D(x) = 3x^{-3} \int dx x^4 \exp(x)/[\exp(x)-1]^2$, and the electron contribution in the form of two systems with level splitting frequencies corresponding to T_1 and T_2 :

$$c_{\text{el}}/R = b_1 \text{Sh}(T_1/T) + b_2 \text{Sh}(T_2/T), \quad (4)$$

$$\text{Sh}(x) = x^2 \exp(x)/[\exp(x) + 1]^2. \quad (5)$$

This very simple model allows a satisfactory description of experimental results for the as-grown and irradiated samples. The cut-off temperature θ_2 decreases from 1845 K for the as-grown diamond to 1735 and 1700 K for the samples irradiated to fluences $\Phi = 2 \times 10^{20}$ and $5 \times 10^{20} \text{ cm}^{-2}$, respectively. The low-frequency part of the phonon spectrum also softens as a result of irradiation, and the vibrational density of states (VDOS) in this region increases approximately by a factor of 2. The T_1 and T_2 values are close to 5 and 20 K, respectively.

Despite the simplified approach, it allows a quite accurate separation of the phonon and electron contributions because the former dominates in the temperature range $T > 40$ K and the latter at $T < 15$ K (Fig. 3). Certainly, the parameters T_1 and T_2 have no well defined values, but the model gives an opportunity to calculate the electron system entropy,

$$S = R \ln 2(b_1 + b_2), \quad (6)$$

and, thus, to find the concentration of two-level systems $c_{\text{TL}} = b_1 + b_2$. This gives 0.9% and 0.8% for the samples irradiated to fluences of 2×10^{20} and $5 \times 10^{20} \text{ cm}^{-2}$, respectively.

Diamond is the wide band-gap semiconductor ($E_g \approx 5.5$ eV). The resistivity ρ of as-grown polycrystalline CVD diamond at room temperature is on the order of $10^{12} - 10^{14} \Omega \text{ cm}$.²⁴ In irradiated samples, ρ drops to $(2-4) \times 10^6 \Omega \text{ cm}$, displaying an activation-type dependence. The formal fitting of ρ at higher temperatures gives the activation energy $E_a \approx 0.3$ eV. The Hall coefficient R_H is relatively small in the explored temperature range, within which the measurements with a reasonable accuracy were possible. The Hall mobility $\mu_H = R_H/\rho$ is also extremely low, $|\mu_H| < 0.1 \text{ cm}^2/(\text{V s})$, which indicates that electron transport takes place across the impurity-type band (via localized states), without an essential activation of carriers in the high mobility bands.

The reduced Raman spectra $I_R(E) = I(E)E/\{E_{\text{sc}}^4[1+n(E)]\}$ [where $I(E)$ is the measured spectrum, E_{sc} is the scattered light energy, and $n(E)$ is the Bose-Einstein factor], together with the two-step Debye spectrum for as-grown and irradiated samples, are shown in Fig. 4.

For the as-grown sample, only one optical mode, the narrow first-order peak at $E = 165$ meV is present. The extended spectrum in the range of 20–170 meV, observed for the neutron-irradiated sample and corresponding to VDOS, is in good agreement with Raman data for ion-irradiated

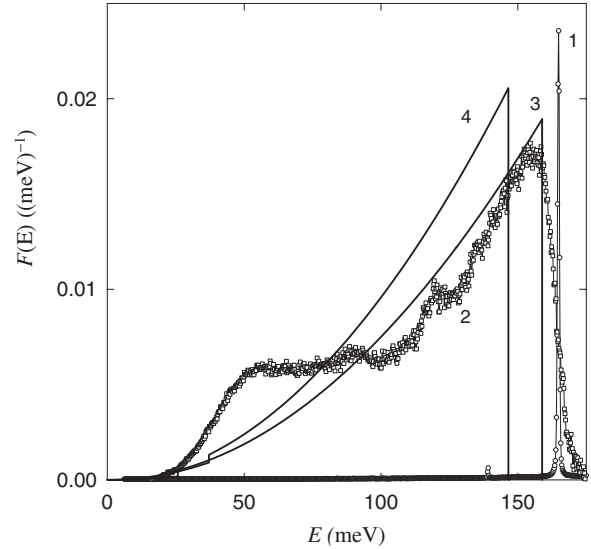


FIG. 4. “Phonon spectrum” $F(E)$ of CVD diamond. The squares are reduced Raman spectra for as-grown $\Phi = 0$ (1) and irradiated $\Phi = 5 \times 10^{20} \text{ cm}^{-2}$ sample (2). The lines are the two-step Debye model: (3) $\Phi = 0$ and (4) $\Phi = 5 \times 10^{20} \text{ cm}^{-2}$.

diamonds.^{8–11} The appearance of such spectra with completely vanished first-order diamond Raman peak at 165 meV (at all fluences used here) is commonly referred to diamond amorphization,²⁵ reaching at vacancies concentration of about $1 \times 10^{22} \text{ cm}^{-3}$.¹⁰ New very broad peaks that appeared are centered at 49 meV (400 cm^{-1}), 119 meV (960 cm^{-1}), 154 meV (1240 cm^{-1}), and 200 meV (1615 cm^{-1}). However, our neutron-diffraction patterns clearly confirm the diamond lattice survived even at highest fluence of $5 \times 10^{20} \text{ cm}^{-2}$, so the Raman spectra reflecting the VDOS are due to a strong disorder in still the crystalline diamond state. The significant atomic displacements from the equilibrium state under irradiation can be accompanied with sp^2 -carbon bond formation as evidenced by a peak at 200 meV.^{8–10}

We conclude that under low-temperature ($T_{\text{irr}} = 325$ K) irradiation with fast neutrons, the diamond crystal structure remains stable at $\Phi \leq 5 \times 10^{20} \text{ cm}^{-2}$. The radiation defects lead to formation of deep electron levels with concentration slightly lower than 1% that carry a magnetic moment and form a multilevel system with splitting on a meV scale. This is in agreement with numerical calculations of band structure,²⁶ which showed that, in particular, a vacancy forms localized electron levels in the diamond band structure close to the middle of the gap, having a magnetic moment of $2\mu_B$ per vacancy.

The authors are thankful to A. V. Saveliev and S. V. Voronina for sample preparation. The work was carried out with partial financial support of Basic Research Program of Presidium of RAS: “Quantum Macrophysics” and “Effect of Atomic-Crystal and Electron Structure on Condensed Matter Properties,” RFBR Grants No. 07-02-00020, No. 07-02-00259, and No. 08-02-00437 and State Contract No. 02.518.11.7026.

*karkin@uraltc.ru

- ¹A. E. Karkin and B. N. Goshchitskii, *Phys. Part. Nucl.* **37**, 807 (2006).
- ²F. Banhart, *Rep. Prog. Phys.* **62**, 1181 (1999).
- ³M. Zaiser, Y. Lyutovich, and F. Banhart, *Phys. Rev. B* **62**, 3058 (2000).
- ⁴J. Isberg, J. Hammersberg, E. Johansson, T. Wikström, D. J. Twitchen, A. J. Whitehead, S. E. Coe, and G. A. Scarsbrook, *Science* **297**, 1670 (2002).
- ⁵C. J. H. Wort and R. S. Balmer, *Mater. Today* **11**, 22 (2008).
- ⁶Y. Takano, M. Nagao, I. Sakaguchi, M. Tachiki, T. Hatano, K. Kobayashi, H. Umezawa, and H. Kawarada, *Appl. Phys. Lett.* **85**, 2581 (2004).
- ⁷V. A. Sidorov, E. A. Ekimov, S. M. Stishov, E. D. Bauer, and J. D. Thompson, *Phys. Rev. B* **71**, 060502(R) (2005).
- ⁸D. T. Morelli, T. A. Perry, and J. W. Farmer, *Phys. Rev. B* **47**, 131 (1993).
- ⁹J. D. Hunn, S. P. Withrow, C. W. White, and D. M. Hembree, *Phys. Rev. B* **52**, 8106 (1995).
- ¹⁰J. O. Orwa, K. W. Nugent, D. N. Jamieson, and S. Prawer, *Phys. Rev. B* **62**, 5461 (2000).
- ¹¹V. D. Blank, V. V. Aksenonkov, M. Yu. Popov, S. A. Perfilov, B. A. Kulnitskiy, Ye. V. Tatyannin, O. M. Zhigalina, B. N. Mavrin, V. N. Denisov, A. N. Ivlev, V. M. Chernov, and V. A. Stepanov, *Diamond Relat. Mater.* **8**, 1285 (1999).
- ¹²P. W. Levy and O. F. Kammerer, *Phys. Rev.* **100**, 1787 (1955).
- ¹³E. R. Vance, *J. Phys. C* **4**, 257 (1971).
- ¹⁴V. Yu. Karasov, S. N. Shamin, V. A. Nikolaenko, E. Z. Kurmaev, and S. V. Shulepov, *Sov. Phys. Solid State* **26**, 2873 (1984).
- ¹⁵N. A. Poklonski, T. M. Lapchuk, N. I. Gorbachuk, V. A. Nikolaenko, and I. V. Bachuchin, *Semiconductors* **39**, 894 (2005).
- ¹⁶S. S. Agafonov, V. P. Glazkov, V. A. Nikolaenko, and V. A. Somenkov, *JETP Lett.* **81**, 122 (2005).
- ¹⁷V. G. Ralchenko, A. A. Smolin, V. I. Konov, K. F. Sergeichev, I. A. Sychev, I. I. Vlasov, V. V. Migulin, S. V. Voronina, and A. V. Khomich, *Diamond Relat. Mater.* **6**, 417 (1997).
- ¹⁸S. Talapatra, P. G. Ganesan, T. Kim, R. Vajtai, M. Huang, M. Shima, G. Ramanath, D. Srivastava, S. C. Deevi, and P. M. Ajayan, *Phys. Rev. Lett.* **95**, 097201 (2005).
- ¹⁹P. Esquinazi, D. Spemann, R. Hohné, A. Setzer, K. H. Han, and T. Butz, *Phys. Rev. Lett.* **91**, 227201 (2003).
- ²⁰J. H. E. Griffiths, J. Owen, and I. M. Ward, *Nature (London)* **173**, 439 (1954).
- ²¹P. W. Whippey, *Can. J. Phys.* **50**, 803 (1972).
- ²²F. Beuneu, C. l'Huillier, J. P. Salvetat, J. M. Bonard, and L. Forro, *Phys. Rev. B* **59**, 5945 (1999).
- ²³A. V. Rode, E. G. Gamaly, A. G. Christy, J. G. Fitz Gerald, S. T. Hyde, R. G. Elliman, B. Luther-Davies, A. I. Veinger, J. Androulakis, and J. Giapintzakis, *Phys. Rev. B* **70**, 054407 (2004).
- ²⁴V. Polyakov, A. Rukovishnikov, B. Garin, L. Avdeeva, R. J. Heidinger, V. Parshin, and V. Ralchenko, *Diamond Relat. Mater.* **14**, 604 (2005).
- ²⁵R. Shuker and R. W. Gammon, *Phys. Rev. Lett.* **25**, 222 (1970).
- ²⁶Y. Zhang, S. Talapatra, S. Kar, R. Vajtai, S. Nayak, and P. M. Ajayan, *Phys. Rev. Lett.* **99**, 107201 (2007).